

Article

Implementation of Resilient Self-Healing Microgrids with IEC 61850-Based Communications

Junho Hong ^{1,*}, Dmitry Ishchenko ² and Anil Kondabathini ²

¹ Department of Electrical and Computer Engineering, University of Michigan-Dearborn, Dearborn, MI 48375, USA

² Hitachi ABB Power Grids, Raleigh, NC 27606, USA; dmitry.ishchenko@hitachi-powergrids.com (D.I.); anil.kondabathini@hitachi-powergrids.com (A.K.)

* Correspondence: jhwr@umich.edu

Abstract: Due to the high penetration of distributed energy resources (DER) and emerging DER interconnection and interoperability requirements, fast and standardized information exchange is essential for stable, resilient, and reliable operations in microgrids. This paper proposes fast fault detection, isolation, and restoration (F-FDIR) for microgrid application with the IEC 61850 Generic Object Oriented Substation Event (GOOSE) communication considering the communication/system failure. GOOSE provides a mechanism for lightweight low latency peer-to-peer data exchange between devices, which reduces the restoration time compared to conventional client-server communication paradigm. The proposed mitigation method for the communication/system failure can find an available restoration scenario and reduce the overall process time. Hardware-in-the-loop (HIL) testbed is designed and implemented with real time digital simulator, microgrid control system, and protection and control intelligent electric devices (IEDs) for the validation. The experimental results show that the proposed F-FDIR and IEC 61850 models can enhance the reliability and interoperability of the microgrid operation and enable self-healing microgrids.

Keywords: microgrids; IEC 61850; Self-healing microgrids; fault detection; isolation and restoration; IEC 61850 based DERs



Citation: Hong, J.; Ishchenko, D.; Kondabathini, A. Implementation of Resilient Self-Healing Microgrids with IEC 61850-Based Communications. *Energies* **2021**, *14*, 547. <https://doi.org/10.3390/en14030547>

Received: 15 December 2020

Accepted: 15 January 2021

Published: 21 January 2021

Publisher's Note: MDPI stays neutral with regard to jurisdictional claims in published maps and institutional affiliations.



Copyright: © 2021 by the authors. Licensee MDPI, Basel, Switzerland. This article is an open access article distributed under the terms and conditions of the Creative Commons Attribution (CC BY) license (<https://creativecommons.org/licenses/by/4.0/>).

1. Introduction

The use of standards-based engineering brought many benefits to power system industry. For instance, IEC 61850 based engineering can (1) reduce the cost of configuration, installation and commissioning, (2) enhance the multi-vendor interoperability, (3) increase the long term stability, and (4) reduce the impact on the existing utility automation systems by upgrading the device capabilities through changing the communication stack in the system (e.g., only need to change the communication stack of the product when revised specific communication service mapping for IEC 61850 models, e.g., MMS, Layer 2 or Layer 3 GOOSE is available) [1]. Furthermore, there are many on-going activities to bridge the conventional industrial communications (Sunspec Modbus, IEC 60870-5-104 and DNP3) to IEC 61850. Therefore, not only the substation automation systems but also many other power system areas have used and can benefit from the IEC 61850 based standardization, especially when it comes to the unified modeling approach. The IEC has released distributed energy resources (DER) related standards (e.g., IEC 61850-7-420 [2] and IEC 61850-90-7 [3]) and they are currently being updated to second edition. These extended standards contain the IEC 61850 model and implementation guidelines for distributed energy resources, e.g., photovoltaics (PV), wind, battery energy storage systems, flywheel, and diesel generator [4]. However, most existing DERs are not yet equipped with IEC 61850 communication interface since (1) the IEC 61850 standards for DERs were not available when they were released to the market and (2) motivation to use the IEC 61850 equipped DERs by the end users at that moment was lacking. Furthermore, currently there

are many different types of DERs available, and it is becoming increasingly complex to integrate and manage all variety within a single management system, e.g., distributed energy resource management system (DERMS) or distribution management system (DMS), so the interoperability problem has risen [5].

Fault detection and isolation is crucial to maintaining a healthy power grid at all levels, e.g., transmission, distribution and microgrids. Extended exposure to fault currents can damage power grid components including costly transformers and circuit breakers. The addition of distributed energy resources to the power grid necessitates new methodology for fault detection and isolation. While existing power grids with a radial distribution structure only have fault current flowing in one direction, power grid with DERs may have fault currents flowing in multiple directions from various power sources. In this regard, the existing power grid control systems suffer from several shortcomings and disadvantages. There remain unmet needs, including increasing fault detection accuracy and speed, improving overall system reliability, and decreasing outage time. For instance, the presence of fault currents from multiple power sources in an active distribution network may cause current control systems to misinterpret the magnitude and direction of fault currents and, therefore the location or existence of a fault. Furthermore, inaccurate fault detection and prolonged exposure to fault currents may also reduce the DER service life. There is a significant need for the unique apparatus, methods, systems and fast techniques for microgrids self-healing. Recent studies showed different type of algorithms attempting to solve these problems [6–13]. A transformative architecture for the normal operation and self-healing of networked microgrids is proposed in [6]. The neighboring islanded microgrids connected through a normally open switch have been used for the development of a self-healing strategy [7]. The authors of [8] considered both dispatchable and non-dispatchable distributed generators (DGs) for the self-healing strategy of microgrids using sectionalizing. In order to enhance the resiliency of microgrids during fault conditions, multi-agent-based system design and automated algorithm have been proposed in [9]. A sequential service restoration (SSR) framework is proposed to generate restoration solutions for distribution systems and microgrids in the event of large-scale power outages [10]. Distributed machine learning based self-healing method is proposed to detect the dynamic signatures of different power system events and tested in offline mode [11]. Centralized protection has also been proposed and validated through real-time simulation studies based on the hardware in the loop approach [12]. Reference [13] introduced the optimal placement of remote-controlled switches to enhance system restoration capacity in order to restore more loads within the DER connected distribution system. Decentralized Multi-Agent-Based Approach has been proposed to restore the low voltage microgrid system [14]. A state-of-the-art protection schemes developed for DC Microgrids in terms of system configurations, fault detection, location, isolation and restoration [15]. A comprehensive review of the microgrid fault diagnosis techniques have studied including artificial neural network (ANN) algorithm [16].

However, there are some concerns for these methods: (1) industrial communications and hardware platforms processing times are not considered, (2) interoperability problems between different vendors' products are not addressed, (3) provisions for communication or device failures that may occur during the FDIR process are not typically made and (4) practical experiment results to identify both application and communication delays using hardware in the loop testbed.

This paper proposes a method to implement GOOSE communication for the system restoration of microgrids, and the software or hardware-based IEC 61850 integration for the existing/new DERs that lack the capabilities both in terms of semantic object models as well as the specific communication service mappings to IEC 61850 MMS and GOOSE communications. Furthermore, communication performance has been tested with protection and restoration algorithms. The main contributions of this paper are (1) fast fault detection, and isolation and restoration algorithm that can be used for a multi-microgrid system, (2) FDIR process considering communication/system failure

using heartbeat signals of GOOSE, and (3) hardware-in-the-loop testbed validation with commercial hardware and industrial communication. Through the combination of the proposed features, the solutions and algorithms can be implemented into a utility system directly. In the remaining of this paper, Section 2 describes IEC 61850 Modeling and System Structure. The fast fault detection, and isolation and restoration algorithm has been proposed in Section 3. Section 4 provides the hardware-in-the-loop testbed and Section 5 provides test results using HIL testbed of the proposed methods and algorithms. Conclusions and recommendations for future work are given in Section 6.

2. IEC 61850 Modeling and System Structure

Figure 1 and Table 1 illustrates the schematic diagram and logical nodes (LNs) of the IEC 61850 models for DERs. In order to get status and send control command for circuit breakers (e.g., point of interconnection (POI), tie and loads) FD1SW adapter contains CSWI and XCBR LNs for breaker control and status, respectively. CSWI handles breaker operation through automated functions, e.g., select before operate (SBO). Following this model, a controller (e.g., FD1SW adapter) will first send a “select” command, to which the outstation device (e.g., circuit breaker) will respond and then, if the outstation device does not receive the “operate” command within a specified amount of time, it will not execute the control action. FD1PV1 represents the photovoltaic (PV) DER adapter and it contains DRCC, DOPM, MMXU and several other LNs. The DRCC logical node represents a supervisory control that covers DER start/stop, and setpoint change (active/reactive power, frequency offset and fixed voltage level). DOPM provides settings for the operating modes changes at the electrical connection point (ECP). More than one mode can be set simultaneously for certain logical combinations, e.g., P-V (active power and voltage), P-Q (active power and reactive power), or HzW. Since MMXU contains measurement data, most of DERs should have this LN for measurement reporting purpose. FD1WG1 is the wind generator DER adapter and it contains WAPC and WRPC. Where WAPC is for wind power plant active power control and WRPC is for wind power plant reactive power control. FD2MCDG1 is the diesel generator adapter and its LNs are similar to PV adapter. FD2BESS1 is the battery energy storage system adapter and its LNs are similar as PV adapter except for DBAT and DRCS. DBAT covers the battery system characteristics required for remote monitoring and control of battery system functions and states, e.g., actual or usable state of charge. DRCS LN defines the control status of one DER unit or aggregations of one type of DER device with a single controller. In this paper, it will be used to check the charge status of a BESS device. For instance, the value of DRCS. ChaSt.stVal 2, 3, 4 and 5 indicate “fully discharged,” “discharged,” “charged,” and “fully charged,” respectively.

Table 1. Logical nodes for Figure 1.

Logical Node Name	Description	Standard
FD1SW	Switches adapter in the feeder 1	Custom
CSWI	This LN class shall be used to control all switching conditions above process level	IEC 61850-7-4
XCBR	This LN is used for modelling switches with short circuit breaking capability.	IEC 61850-7-4
FD1PV1	Photovoltaic (PV) DER adapter	Custom
DRCC	The DER supervisory control logical node defines the control actions for one DER unit or aggregations of one type of DER device with a single controller.	IEC 61850-7-420
DOPM	This logical node provides settings for the operating mode at the electrical connection point.	IEC 61850-7-420

Table 1. Cont.

Logical Node Name	Description	Standard
MMXU	This LN shall be used for calculation of currents, voltages, powers and impedances in a three-phase system.	IEC 61850-7-4
FD1WG1	Wind generator DER adapter	Custom
WAPC	This logical node shall comprise the data classes that represent information concerning wind power plant active power control.	IEC 61400-25-2
WRPC	This logical node shall comprise the data classes that represent information concerning wind power plant reactive power control.	IEC 61400-25-2
FD2MCDG1	Diesel generator adapter	Custom
FD2BESS1	Battery energy storage system adapter	
DBAT	The DBAT logical node covers the battery system characteristics covered in the DBAT logical node reflect those required for remote monitoring and control of critical auxiliary battery system functions and states.	IEC 61850-7-420
DRCS	The DER controller DRCS logical node defines the control status of one DER unit or aggregations of one type of DER device with a single controller.	IEC 61850-7-420

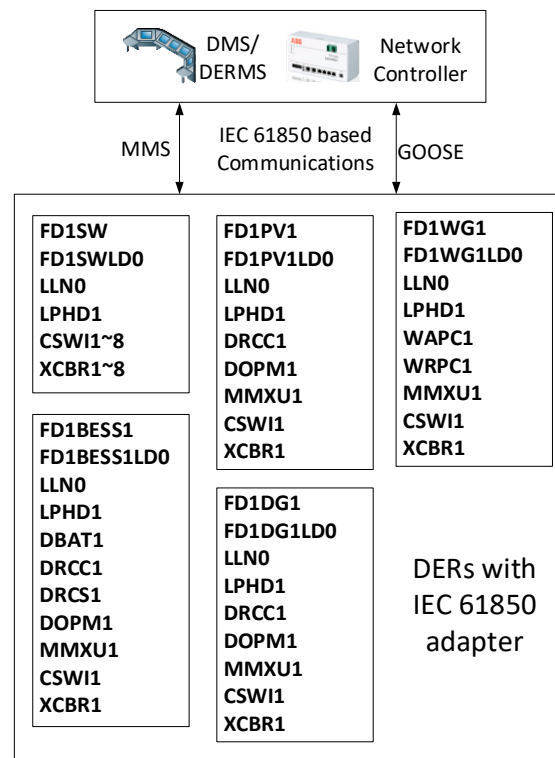


Figure 1. Logical nodes of IEC 61850 based adapters for each Distributed Energy Resource (DER) and breaker.

3. F-FDIR

Conventional distribution systems with no DER usually have a radial structure. In this case, when a distribution line fault occurs, the fault current always flows to the one direction, e.g., from substation (source) to the fault location. Utilities implement fault detection, isolation and restoration (FDIR) functions by integrating overcurrent relays, reclosers, sectionalizers and fuses. However, as already mentioned, increased penetration of DERs in the distribution system (e.g., microgrid) introduces bi-directional load currents, reduced fault currents or meshed structure. Hence, in some cases, it is hard to use conventional ways to detect, isolate and restore the service after a fault in the distribution system, especially with multiple DER units. This section presents the fast fault detection, isolation and restoration (F-FDIR) algorithm using the proposed standard-based communication adapter. The following assumptions are made:

1. The target networked microgrid system is operating in a grid-connected mode.
2. The target system has a communication backbone system, e.g., wireless or wired.
3. Each switch has a communication capability to send measurements (e.g., currents and voltages) and receive control commands.
4. Each switch may have a capability to interrupt the load currents.
5. Each switch may have a directional fault indicator (DFI) capability, or they can receive the DFI information from the external DFI devices.
6. Each subsystem has its own network-controller (i.e., microgrid controller) for monitoring, control and settings change as shown in Figure 2.
7. The network-controllers of each subsystem can communicate with each other.
8. The standard-based communications (e.g., GOOSE and MMS) can be encrypted and/or authenticated as described in IEC 62351 standard series for enhanced cyber security [17–19].

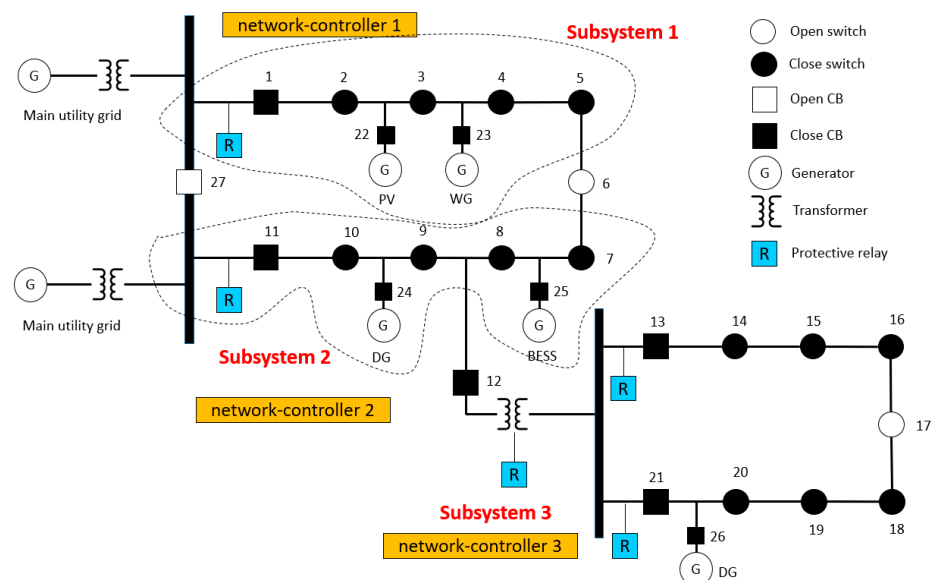


Figure 2. Single line diagram of the microgrid system.

Please note that the proposed F-FDIR algorithms are based on the grid-connected microgrid system with high penetration of distributed energy resources and communication capability. Thus, if one of the assumptions does not meet the requirement, the proposed F-FDIR algorithm cannot show the optimal results. The F-FDIR algorithm is comprised of several steps. The first step is to detect fault location using directional fault indicators (DFI). During the normal operation of microgrids, the network controllers (as shown in Figure 2) are periodically collecting field data (e.g., voltages, currents, and phasors) from switches and sensors via wired or wireless communications either through polling or

GOOSE peer-to-peer mechanisms (e.g., using heartbeat signals) [20–23]. When a fault occurs at a feeder, the protective IED picks up the fault. Then the IED sends a trip signal to the feeder circuit breaker in order to clear the fault according to the associated time-current curve (e.g., GOOSE re-transmission scheme). The fault information will be transferred to both the switches and network controllers within a microgrid. Once microgrid switches receive the fault indication information from the IED reporting a fault, they will broadcast the pre- and post-fault conditions that include the measurements, status and DFI to the corresponding network controller. Then, the microgrid network controller checks the status of CBs and switches.

Figure 3 shows possible DFI combinations when a fault has occurred on a different section of the microgrid feeder. For instance, a feeder without DER (case 1) is a conventional radial distribution feeder. Due to the unidirectional characteristic of the radial feeder, the direction of load flow is always from a source (upstream) to loads (downstream). In this case, if a fault occurs, the fault indicators will show the location of the fault (SW1 saw the fault but SW2 could not). In contrast, the DER integrated microgrid shows a bidirectional characteristic of load flows, as illustrated in the Figure 3 (case 2 and case 3). In these cases, the location of fault can be identified the fault indicators where they are pointing at the same location (e.g., FIs of POI CB and SW1 are pointing out the same location). After receiving the status information from switches, the network controller will calculate the location of the faulted section using topological analysis (i.e., multi-agent based de-centralized) and Algorithm 1 sequentially lists all the detailed steps. D_{pre} and D_{post} contain directional fault indicators (DFI) information of each switch or breaker to identify the fault location for the DER integrated microgrid.

Algorithm 1. Topology Based Fault Location Detection

```

1 Input: Measurements and statuses of field devices, information from protective IEDs, and DFIs from switches
2 Output: Location of the faulted section within the microgrid feeder
3 STATUS( $SW_c(i, t)$ ,  $SW_v(i, t)$ ,  $SW_{st}(i, t)$ ,  $SW_{dfi}(i, t)$ ,  $CB_c(i, t)$ ,  $CB_v(i, t)$ ,  $CB_{st}(i, t)$ ,  $CB_{dfi}(i, t)$ )
    $\rightarrow N_{ctr,ij}$ 
4 if ( $IED_{tr}(i, t) = true$ ) then
5   Calculate topology-based fault location detection,  $N_{ctr,ij} \rightarrow FD(STATUS(M_{sw,i}, M_{cb,i}))$ 
6   for 1: Number of switches do
7      $D_{pre} = get(\text{before the event}, STATUS(t^-))$ 
8      $D_{post} = get(\text{after the event}, STATUS(t^+))$ 
9   End
10  Check DFIs ( $D_{pre}, D_{post}$ );
11  if (DFIs are pointing same direction) then
12    Fault at the next section of the last DFI
13  elseif (DFIs are pointing same point of section) then
14    Fault at the pointing section
15  end
16 end

```

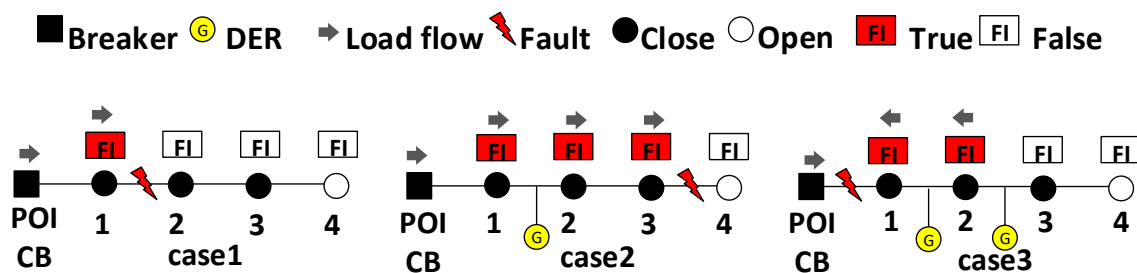


Figure 3. Examples of possible combination of directional fault indicators (DFIs) for the microgrid feeder.

The second step is to isolate the faulted section for the restoration process. After the faulted section in Algorithm 1 has been identified, the supervisory network controller checks for the latest status of the corresponding switch or breaker and issues an open command. Once switches or breakers have changed their status, they will report back to the network controller for the confirmation. However, due to the possible communication errors, device failure or abnormal behavior of the system equipment, the normal operation of isolation may be interrupted so the device is not able to participate in the F-FDIR process. The proposed faulted section isolation (FSI) algorithm checks the measurement and communication heartbeat in order to identify the problems when the expected outcome is not available from the field devices. If there is any device-communication-failure problem, the FSI will extend the isolation section by choosing the nearest switch or breaker within the solution sets, it can maintain the similar process time even though there is a failure during the F-FDIR process. For instance, the faulted section has been identified between POI CB and SW 1 in the case 3 of Figure 3. However, SW 1 is not operating after a couple of tries of opening attempts. Then the proposed FSI will extend the isolation section up to SW 2 and isolate sections POI CB through SW2. In the meantime, the FSI tries to open the SW of the DER since it is within the faulted section. Similarly, if SW of the DER is not operating, the FSI will send the reducing power order command (i.e., minimum) to the DER in order to reduce the impact of the fault. This will create an unwanted outage section but it can still reduce the outage time. The following Algorithm 2 shows more details step-by-step.

Algorithm 2. Faulted Section Isolation

1 **Input:** Measurements and statuses of field devices, and status feedback from the switches and DERs
Output: Isolation of faulted section within microgrids
2 **STATUS**($SWc(i, t)$, $SWst(i, t)$, $CBc(i, t)$, $CBst(i, t)$) $\rightarrow N_{ctr,ij}$
3 Check the status of the target CB and switches: $SWst(i, t)$, $CBst(i, t)$
4 **if** ($(SWst(i, t) = \text{close}) \wedge (CBst(i, t) = \text{close})$) **then**
5 Send open command to SW i and CB i
6 **if** ($(SWst(i, t) = \text{open}) \wedge (CBst(i, t) = \text{open})$) **then**
7 **else**, check **if** ($(SWc(i, t) = 0) \wedge (CBc(i, t) = 0)$) **then**
8 re-send open command to SW i and CB i
9 Check the heartbeat of SW i and CB i : $SWhb(i, t)$, $CBhb(i, t)$
10 **if** ($(SWhb(i, t) = \text{false}) \vee (CBhb(i, t) = \text{false})$) **then**
11 Extend the isolation section, and then send open command to SW $i \pm 1$ and CB $i \pm 1$
12 Go back to step 6, repeat N times
13 **End**
14 **End**
15 **End**
16 **if** DER exists within the faulted section **then**
17 Send open command to SW i
18 **if** $SWst(i, t) = \text{close}$ **then** reduce power order of DER i to min. set $DERpo(i, t) = \text{minimum}$
19 **End**
20 **End**

The final (third) step is to restore the remaining healthy sections (SIM7_FD1NC1LD0/LLN0\$Fdir2). If the fault is not between the point of interconnection (POI) CB and the adjacent switch, the close switching command is sent to the POI CB for the restoration (i.e., re-supplying power to the outage area). If this process creates any islands within nested microgrid system, network controllers or other devices need to check whether current total generation is higher than the total loads within each subsystem island (SIM7_FD1NC1LD0/LLN0\$Confirmation). If that is the case and if there is any DER within subsystem islands, check whether they can support their own local loads while considering DER output setpoint adjustments as needed. If the total generation within subsystem island cannot support the total local loads, network-controller will ask to other

network-controllers whether it can transfer the loads to them. If there is any critical load within subsystem islands, the network controller calculates whether it can restore the critical load (SIM8_FD2NC2LD0/LLN0\$Confirmation). In this process, partial load transfer to another subsystem and local load shedding need to be considered. When transferring the partial load and it is directly connected to a DER, synchronization should be considered. If there are any operating DERs within subsystem island and they cannot support loads, the network-controller sends an open command to the DER controller so that the repair crews can be safely dispatched. In the case when there is any operating DER within the subsystem island, it can be transferred to another subsystem. After the automated outage restoration process is finished, it is required to dispatch a field crew for the physical restoration of faulted location. The details of system restoration algorithms are illustrated in Algorithm 3 as follows.

Algorithm 3. System restoration

```

1 Input: Measurements and statuses of field devices, and status feedback from the switches and DERs
Output: Restoration of healthy section within microgrids
2 STATUS( $SWst(i, t)$ ,  $CBst(i, t)$ ,  $LOADpq(i)$ ,  $DERca(i)$ ,  $N_{ctr,ij}^{gen}$ )  $\rightarrow N_{ctr,ij}$ 
3 Restore healthy upstream section (exception applied: 1-1, 2-1, ... 8-1)
4 if island exists then
5   if island has DER then
6     if  $\sum LOADpq(i) \text{ island} > \sum DERca(i) \text{ island}$  then
7       if  $\sum N_{ctr,ij}^{gen} > \sum LOADpq(i) \text{ island}$  then transfer loads
8       else then check critical load within island
9         if  $\sum LOADpq(i) \text{ critical, island} > \sum N_{ctr,ij}^{gen}$  after load shedding then pick up critical loads
10        end
11      end
12    else then (1) shedding DERs within island or
13    (2) transfer DERs to another subsystem
14    end
15  else restore remaining healthy loads (steps 7~11)
16  end
17 End

```

Therefore, the proposed F-FDIR framework can enhance the resiliency of microgrid system by reducing system restoration time using the proposed algorithms, e.g., considering communication failure and fast communications between devices.

4. HIL Testbed

A cyber-physical testbed is critical for the study of cyber-physical behavior of power systems. For reason of security by power companies, real measurements (e.g., voltages, currents and binary status) and ICT data (e.g., communication protocols, system logs, and security logs) are not available. A testbed is a good alternative to acquire realistic cyber (i.e., ICT data) and physical (i.e., power system measurements) system data for research and demonstration purposes. The cyber-physical testbed provides a realistic environment to study the interactions between a complex power system and the ICT system. To validate the proposed algorithms in a realistic environment, a time-domain electromagnetic transient power system simulation model has been developed using MATLAB-Simulink Simscape Power Systems (R2017, MathWorks, Natick, MA, USA) and converted to a real-time simulation model suitable for use with the 5600 series OPAL-RT RT-LAB real-time simulation platform [24]. The microgrid model used for the RTHIL simulation is shown in Figure 2. The model is created for a representative medium voltage 13.5 kV grid-connected microgrid and includes a number of controllable loads, 1.5 MVA doubly-fed wind turbine, 1MW/2MWh energy storage producing around 500 kW, 1MW PV plant and a 10 MW diesel generator. Additionally, a low voltage network is also

modeled with a diesel generator connected to the 480 V side. A total of 6 embedded devices (1.2 GHZ quad-core ARM Cortex COTS with 100 Mbps Ethernet) are implemented for IEC 61850 communication adapters. Detailed models for PV, wind and diesel generator control systems have also been developed.

4.1. IEC 61850 Communication Adapter

This paper implemented standard-based (e.g., IEC 61850-7-420 & IEC 61850-90-7) communication adapter for the simulated DERs or distributed generators (DGs) in OPAL-RT RT-LAB. The implemented adapter has the capability to monitor, analyze and control the DERs with standardized communication, e.g., IEC 61850 based generic object oriented substation event (GOOSE), and manufacturing message specification (MMS) as shown in Figure 4. As a prototype implementation, the proposed adapter can map measurements and controls of UDP (user datagram protocol) communication from OPAL-RT RT-LAB with the IEC 61850 stack. Then it will communicate with external platforms that have IEC 61850 based communication and exchange data with the conventional DER controllers. Each analog and digital value of UDP communication are mapped to the corresponding IEC 61850 based LNs and data attributes. Then a distributed energy resource management system (DERMS) with IEC 61850 capability can get measurements and send control messages from/to DERs via MMS and GOOSE, respectively. MMS communication (server is in adapter and client is in human machine interface) is implemented in the communication adapter. Whereas GOOSE publisher and subscriber are also implemented in communication adapter. Once the communication adapter is integrated into the distributed generation (i.e., OPAL-RT RT-LAB), the communication latency needs to be considered since there will be an additional communication paths (e.g., from/to communication adapter to/from network controller). However, due to the characteristic of IEC 61850 based GOOSE (<3 ms) the actual additional communication delays are minimal (latency of UDP protocol is usually <10 ms). It can receive all GOOSE data (status of all microgrid circuit breakers) from the protection relays, and then estimate the mode of operation, e.g., grid connected or islanded mode, in order to implement more reliable microgrid functions. This will also include the sequence of events, and logging functions. The data mapping logic is crucial for the adapter since it enables DER controller and external devices to exchange the data. In this logic, each analog and digital data point is mapped to the corresponding IEC 61850 Logical Nodes and models.

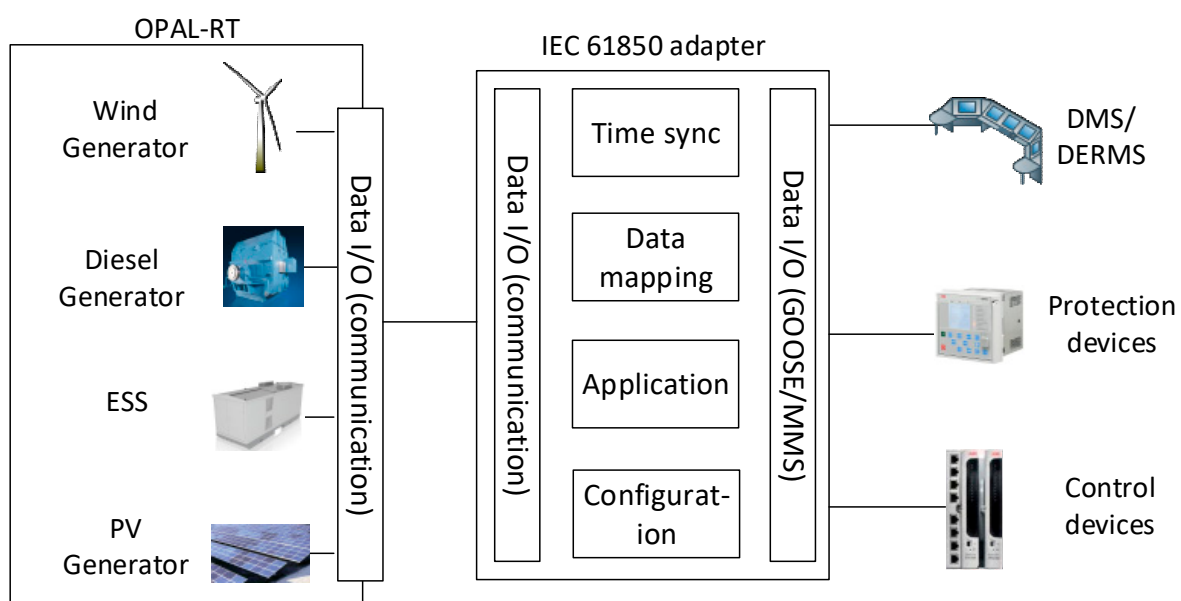


Figure 4. A schematic diagram of the proposed communication adapter for DERs.

4.2. IEC 61850 Based HIL Testbed

An HMI prototype implements supervisory microgrid control logic and is integrated into the HIL system using IEC 61850 communications through the proposed adapters. The controllers that used for the demonstration are (1) microgrid network controller 1 for subsystem 1, (2) microgrid controller 2 for subsystem 2, (3) a communication adapter for DERs, and (4) communication adapter for the circuit breakers and switches. The communication adapters in Figure 5 receive/send UDP communication from/to OPAL-RT and convert it to IEC 61850 communications. For instance, the output from DER controller is simulated in Opal-RT, and the UDP communication is connected to the logic for interface with DERs (i.e., IEC 61850 adapter) as shown in Figure 5. Hence, it can enable HIL system to exchange status and measurement data via GOOSE and MMS messages. The HMI and the microgrid control system control the circuit breakers and the DER in the simulation through GOOSE and MMS can also receive feedback from the real-time simulation in the form of UDP communication, thus completing the closed-loop testing environment.

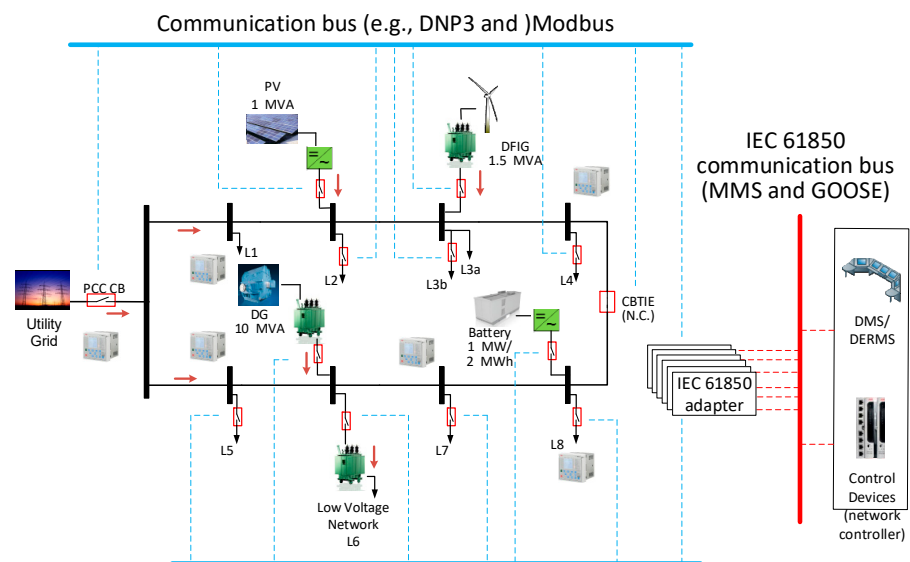


Figure 5. Microgrid HIL Testbed.

5. Case Study

5.1. Case Study 1: Validation of IEC 61850 Adapter

Figure 6 shows the RTHIL simulation results with events, corresponding control commands and system response as indicated in the graph. All measurements and controls are communicated between OPAL-RT and HMI via IEC 61850 adapters (MMS and GOOSE communication).

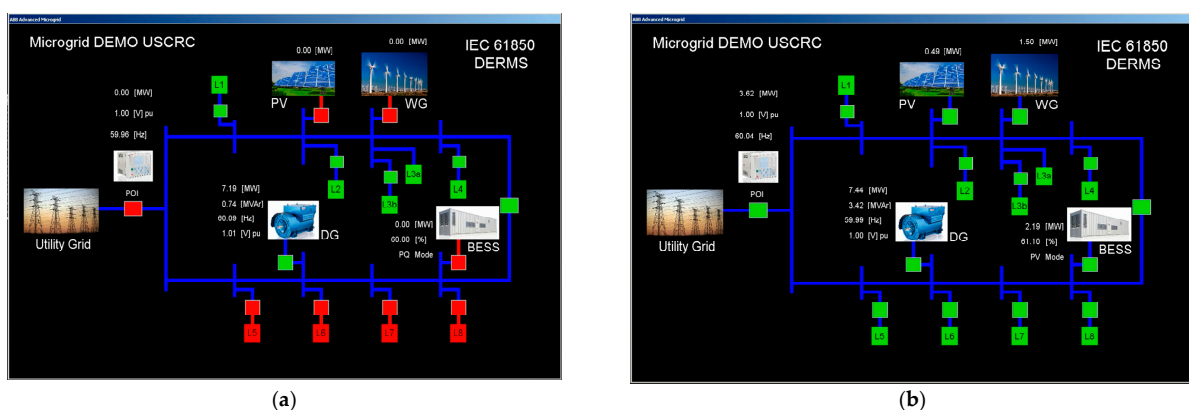


Figure 6. Human machine interface (HMI) prototype: (a) Islanded microgrid, (b) Grid connected microgrid.

The Initial system condition is an unplanned microgrid islanded operation due to the external fault at utility grid, POI breaker tripped and then PV, WG and BESS DERs are also tripped. Please note that green color indicates closed status of breaker whereas red color shows the opened status of breaker in Figure 6a,b.

During the islanded operation of microgrid, the diesel generator is supplying power to some of local loads, e.g., L1, L2, L3 and L4 as shown in Figure 6a. At this time, POI P measurement shows 0 (MW) as illustrated in Figure 6 (POI CB is opened). Once the external fault is cleared, the microgrid will be connected back to the grid with the following sequence of events (Table 2):

Table 2. Validation of IEC 61850 Adapter.

1	The operator sends a close command to POI CB and microgrid is in grid connected mode and receives power from the utility grid as described in Figure 7. SBO command has been issued via SCSWI1.Pos in FD1SW adapter. Then the changed CB status is delivered via XCBR1.Pos.stVal. Please note that in order to show the communication possibility using the proposed adapter, synchronization is not performed in this scenario.
2	PV CB is closed via control command.
3	Wind DER CB is closed. The microgrid is supplying power to the utility grid since it is generating more power than its loads within microgrid. Please note that the transients are due to the absence of re-synchronization function between the microgrid and the wind DER in the simulation model.
4	BESS DER CB is closed. Once BESS is connected to the grid BESS is in charging mode and load flows direction is changed. Now utility grid is supplying power to the microgrid.
5	Load 8 CB is closed.
6	Load 5 and 6 CBs are closed.
7	Battery mode has been changed from charging to discharging. This can be monitored via DRCS1.ChaSt.stVal.
8	Load 7 CB is closed.

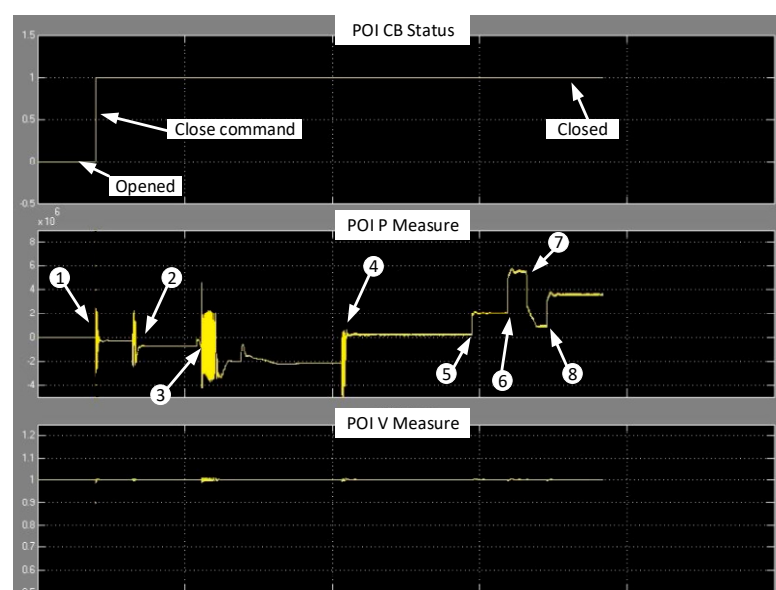


Figure 7. Blackstart case study using IEC 61850 adapter (OPAL-RT screen).

5.2. Case Study 2: F-FDIR

The subsystem 2 in Figure 2 has been used for the case study of F-FDIR. A fault is generated at the section between SW9 and SW10. The following sequence of events (Table 3) describes details of Figures 9 and 10.

Table 3. Validation of F-FDIR.

1	Before this event, microgrids are operating normally as a grid connected mode. When a permanent three-phase to ground fault occurred at the section between SW9 and SW10, the subsystem 2 will experience the transient as shown in the Figure 9 (CB11 voltage and current graph).
2	The protective IED picks up the fault and sends a trip signal to CB11 in the subsystem 2 (the detailed packets have been shown in Figure 8). Then the switches in the subsystem 2 will report the D_{pre} and D_{post} to the network controller 2 as described in Algorithm 1.
3	CB11 opened after receiving the switching control command from protective IED.
4	CB11 clears the fault.
5	The network controller calculates the faulted section based on Algorithm 2, and then sends switching commands to SW 9 and SW10. The SW10 is now opened.
6	SW 9 is now opened by the network controller 2.
7	The fault has been isolated by switching actions; however, the local DER keeps contributing the voltage.
8	The restoration process is started so the network controller 2 is closing CB11 and restore the healthy upstream section.
9	After restoring the upstream section, the sections from main utility grid to SW10 are now energized.
10	The network controller 2 is calculating whether the remaining DER can cover the remaining loads within the island. However, remaining loads are bigger than remaining DER, the network controller 2 and 1 are exchange the data to check whether subsystem 1 can cover the remaining healthy loads in subsystem 2 as illustrated in Algorithm 3. Then the network controller 2 transfers remaining loads to subsystem 1 by closing SW 6 as shown in Figure 9.

```

122 28.259000  Abb0y/Me_21:7c:eb  Iec-Tc57_01:00:00  GOOSE  159
123 28.264929  Abb0y/Me_21:7c:eb  Iec-Tc57_01:00:00  GOOSE  164
124 28.265113  Abb0y/Me_21:7c:eb  Iec-Tc57_01:00:00  GOOSE  164
125 28.267231  Abb0y/Me_21:7c:eb  Iec-Tc57_01:00:00  GOOSE  164
126 28.271496  Abb0y/Me_21:7c:eb  Iec-Tc57_01:00:00  GOOSE  164
127 28.273685  Raspberr_id:a1:9b  Iec-Tc57_01:00:09  GOOSE  191
128 28.273686  Raspberr_id:a1:9b  Iec-Tc57_01:00:09  GOOSE  191
129 28.307027  Raspberr_48:f4:ce  Iec-Tc57_01:00:26  GOOSE  254
130 28.307056  Raspberr_48:f4:ce  Iec-Tc57_01:00:27  GOOSE  176
131 28.307230  Raspberr_48:f4:ce  Iec-Tc57_01:00:25  GOOSE  158
132 28.307301  Raspberr_48:f4:ce  Iec-Tc57_01:00:25  GOOSE  158
> Frame 113: 164 bytes on wire (1312 bits), 164 bytes captured (1312 bits) on interface \Device\NPF_{
> Ethernet II, Src: Abb0y/Me_21:7c:eb (00:21:c1:21:7c:eb), Dst: Iec-Tc57_01:00:00 (01:0c:cd:01:00:00)
< GOOSE
  APPID: 0x3001 (12289)
  Length: 150
  Reserved 1: 0x0000 (0)
  Reserved 2: 0x0000 (0)
  < gosePdu
    gocbRef: AA1J1Q02A1LD0/LLN0$G0$gcbTripSignal
    timeAllowedtoLive: 20000
    dataSet: AA1J1Q02A1LD0/LLN0$TripSignal
    goID: AA1J1Q02A1LD0/LLN0.gcbTripSignal
    t: May 31, 2018 15:00:20.295040190 UTC
    stNum: 2
    sqlNum: 0
    test: False
    confRev: 100
    ndsCom: False
    numDataSetEntries: 1
  < allData: 1 item
    < Data: boolean (3)
      boolean: True

```

Figure 8. Snapshot of generated IEC 61850 messages during F-FDIR process.

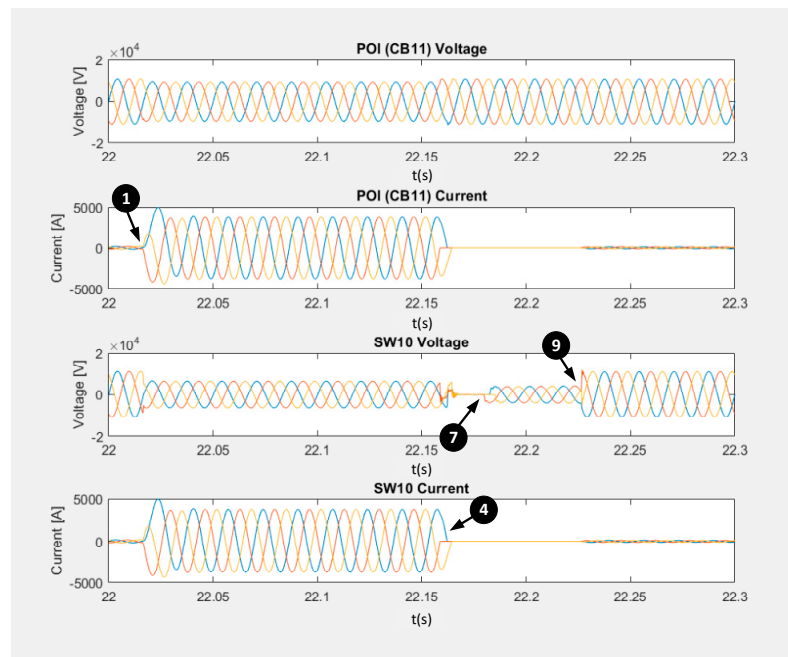


Figure 9. Fast fault detection, isolation, and restoration (F-FDIR) process for a fault between SW9 and SW10.

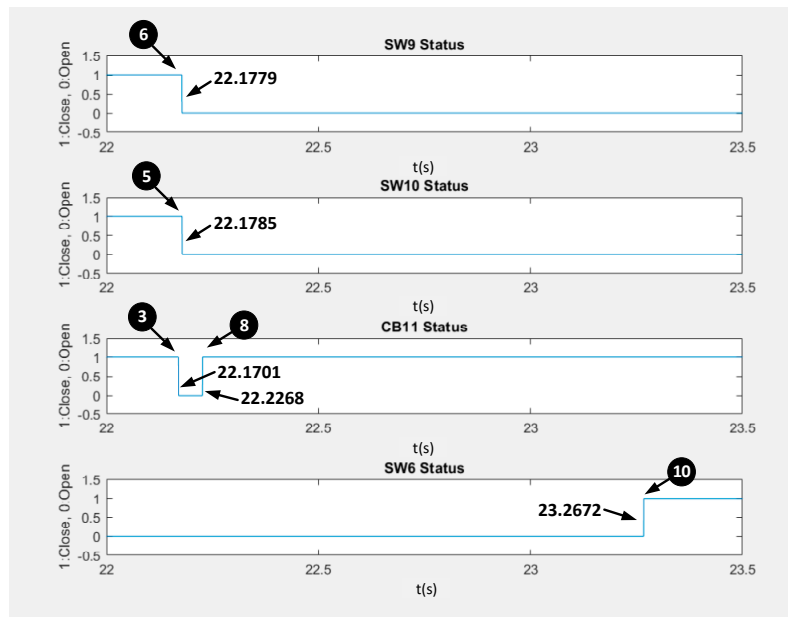


Figure 10. F-FDIR process time using GOOSE communication (including load transfer time between nested microgrids).

As shown in Figure 10, the fault detection and isolation process took around 8 (ms), and then the restoration process to pick up the healthy section in upstream feeder took 48 (ms). Another restoration process to calculate the remaining capacity of DER and loads, communicating with other network controllers, and load transfer switching action took another 1.04 (s).

As shown in Table 4, if there is a device communication failure during the F-FDIR process, the total restoration time can be changed to search the available devices that can participate in the F-FDIR process as follows.

Table 4. Time measurements of fault detection and isolation process. with and without device communication failure mitigation during F-FDIR process (considering GOOSE communication latency).

No.	Normal Scenario	Without Device Communication Failure Mitigation	With Device Communication Failure Mitigation
1	CB11 opened at 22.1701 s	CB11 opened at 22.1701 s	CB11 opened at 22.1701 s
2	SW9 opened at 22.1779 s	SW9 does not response	SW9 does not response
3	SW10 opened at 22.1785 s	SW10 opened at 22.1785 s	SW10 opened at 22.1785 s
4	-	-	Check heartbeat of SW9, 8 and CB 12 at 22.1799 s
5	-	-	SW 8 and CB 12 opened at 22.1819
Total time	8 ms	Fault detection and isolation process failed due to the communication failure	12 ms (4 msec to find the available SW and CB)

6. Conclusions

Microgrids consist of many different types of devices that include protection and control IEDs, sensors and DERs. Microgrids operation is subject to several uncertain factors, e.g., stochastic operation with intermittent fluctuations in renewables, frequent DERs maintenance or shut down. Due to the bi-directional load flow characteristic of DERs integrated into microgrid structure, a conventional protection coordination scheme may not always be applicable. This paper provides a F-FDIR algorithms using the communication adapter that enables standardized communication for existing DERs for monitoring and control purposes (maximize the performance of the proposed F-FDIR, an Ethernet-based communication network is preferred).

The proposed F-FDIR algorithms can identify the location of the faulted section of the microgrid systems. The method is designed to be robust to possible communication/system failures and has been validated by testing with realistic fault and error scenarios using the controller hardware-in-the-loop real-time simulation testbed, e.g., a line fault with/without DERs in the feeder at different locations. For future work, additional functions need to be tested and analyzed, for instance, plug and play (auto-registration) and cloud-based operation. In order to get a more realistic analysis of F-FDIR results, future simulation results need to consider the switching operation and synchronization delays for DER connected section transfer. Furthermore, the developed functions require engineering efforts to integrate with a multi-vendor system and handle more industrial communication protocols (e.g., DNP3 and Modbus) to resolve other potential issues (cybersecurity and wide area network) and need to be tested in the power electronic-based generations for the islanded microgrid.

Author Contributions: Conceptualization, J.H. and A.K.; methodology, J.H.; software, A.K.; validation, J.H., A.K. and D.I.; formal analysis, D.I.; investigation, D.I.; resources, J.H.; data curation, A.K.; writing—original draft preparation, J.H.; writing—review and editing, J.H.; visualization, A.K.; supervision, D.I.; project administration, D.I.; funding acquisition, D.I. All authors have read and agreed to the published version of the manuscript.

Funding: This research was funded by ABB Inc., grant number NMMFII.

Institutional Review Board Statement: Not applicable.

Informed Consent Statement: Not applicable.

Data Availability Statement: The data presented in this study are available on request from the corresponding author.

Conflicts of Interest: The authors declare no conflict of interest.

Abbreviations

$SWc(i, t)$	Measured current of switch i at time t
$SWv(i, t)$	Measured voltage of switch i at time t
$SWst(i, t)$	Status of switch i (st = open or close) at time t
$SWdfi(i, t)$	Directional fault indicator of switch i at time t
$SWhb(i, t)$	Heartbeat (i.e., comm.) of switch i at time t
$CBc(i, t)$	Measured current of CB i at time t
$CBv(i, t)$	Measured voltage of CB i at time t
$CBst(i, t)$	Status of CB i (st = open or close) at time t
$CBdfi(i, t)$	Directional fault indicator of CB i (DFI = true (forward or backward) or false) at time t
$CBhb(i, t)$	Heartbeat (i.e., comm.) of CB i at time t
$LOADpq(i)$	Active and reactive power information of load i
$DERca(i)$	Generation capability of DER i
$SWco(i)$	Control of switch i (open or close)
$CBco(i)$	Control of CB i (open or close)
$IEDtr(i, t)$	Trip signal of IED i (trip = true or false) at time t
D_{pre}	Dataset for before event
D_{post}	Dataset for after event
$N_{ctr,ij}$	Network controller i at microgrid j
$N_{ctr,ij}^{gen(t)}$	Total generation of microgrid j (managed by controller i)
$DERpo(i, t)$	Power order of DER i at time t
$M_{sw,i}$	Measurement set of SW i ($SWc(i, t)$, $SWv(i, t)$, $SWst(i, t)$, $SWdfi(i, t)$)
$M_{cb,i}$	Measurement set of CB i ($CBc(i, t)$, $CBv(i, t)$, $CBst(i, t)$, $CBdfi(i, t)$)

References

- IEC 61850-1. *Communication Networks and Systems for Power Utility Automation—Part 1: Introduction and Overview*, 2nd ed.; IEC: Geneva, Switzerland, 2013.
- IEC 61850-7-420. *Communication Networks and Systems for Power Utility Automation, Part 7-420: Basic Communication Structure—Distributed Energy Resources Logical Nodes*, 1st ed.; IEC: Geneva, Switzerland, 2009.
- IEC 61850-90-7. *Communication Networks and Systems for Power Utility Automation, Part 90-7: Object Models for Power Converters in Distributed Energy Resources (DER) Systems*, 1st ed.; IEC: Geneva, Switzerland, 2013.
- Pei, W.; Qi, Z.; Deng, W.; Shen, Z. Operation of battery energy storage system using extensional information model based on IEC 61850 for micro-grids. *IET Gener. Transm. Distrib.* **2016**, *10*, 849–861. [[CrossRef](#)]
- Khodaei, A. Microgrid Optimal Scheduling with Multi-Period Islanding Constraints. *IEEE Trans. Power Syst.* **2013**, *29*, 1383–1392. [[CrossRef](#)]
- Wang, Z.; Chen, B.; Wang, J.; Chen, C. Networked Microgrids for Self-Healing Power Systems. *IEEE Trans. Smart Grid* **2016**, *7*, 310–319. [[CrossRef](#)]
- Pashajavid, E.; Shahnia, F.; Ghosh, A. Development of a Self-Healing Strategy to Enhance the Overloading Resilience of Islanded Microgrids. *IEEE Trans. Smart Grid* **2017**, *8*, 868–880.
- Wang, Z.; Wang, J. Self-Healing Resilient Distribution Systems Based on Sectionalization Into Microgrids. *IEEE Trans. Power Syst.* **2015**, *30*, 3139–3149. [[CrossRef](#)]
- Khederzadeh, M. Multi-agent system design for automation of a cluster of microgrids. *CIREC Open Access Proc. J.* **2017**, *2017*, 1304–1307. [[CrossRef](#)]
- Chen, B.; Chen, C.; Wang, J.; Butler-Purry, K.L. Sequential Service Restoration for Unbalanced Distribution Systems and Microgrids. *IEEE Trans. Power Syst.* **2018**, *33*, 1507–1520. [[CrossRef](#)]
- Al Karim, M.; Currie, J.; Lie, T.T. Dynamic Event Detection Using a Distributed Feature Selection Based Machine Learning Approach in a Self-Healing Microgrid. *IEEE Trans. Power Syst.* **2018**, *33*, 4706–4718. [[CrossRef](#)]
- Monadi, M.; Gavriluta, C.; Luna, A.; Candela, J.I.; Rodriguez, P. Centralized Protection Strategy for Medium Voltage DC Microgrids. *IEEE Trans. Power Deliv.* **2017**, *32*, 430–440. [[CrossRef](#)]
- Xu, Y.; Liu, C.-C.; Schneider, K.P.; Ton, D.T. Placement of Remote-Controlled Switches to Enhance Distribution System Restoration Capability. *IEEE Trans. Power Syst.* **2016**, *31*, 1139–1150. [[CrossRef](#)]
- Rokrok, E.; Shafie-khah, M.; Siano, P.; Catalão, J.P. A Decentralized Multi-Agent-Based Approach for Low Voltage Microgrid Restoration. *Energies* **2017**, *10*, 1491. [[CrossRef](#)]
- Javed, W.; Chen, D.; Farrag, M.E.; Xu, Y. System Configuration, Fault Detection, Location, Isolation and Restoration: A Review on LVDC Microgrid Protections. *Energies* **2019**, *12*, 1001. [[CrossRef](#)]

16. Fahim, S.R.; Sarker, S.K.; Muyeen, S.M.; Sheikh, R.I.; Das, S.K. Microgrid Fault Detection and Classification: Machine Learning Based Approach, Comparison, and Reviews. *Energies* **2020**, *13*, 3460. [[CrossRef](#)]
17. IEC TS 62351-1:2007. *Power Systems Management and Associated Information Exchange—Data and Communications Security—Part 1: Communication Network and System Security—Introduction to Security Issues*, 1st ed.; IEC: Geneva, Switzerland, 2007.
18. Hong, J.; Nuqui, R.F.; Kondabathini, A.; Ishchenko, D.; Martin, A. Cyber Attack Resilient Distance Protection and Circuit Breaker Control for Digital Substations. *IEEE Trans. Ind. Inform.* **2018**, *15*, 4332–4341. [[CrossRef](#)]
19. Hong, J.; Liu, C.-C. Intelligent Electronic Devices with Collaborative Intrusion Detection Systems. *IEEE Trans. Smart Grid* **2017**, *10*, 271–281. [[CrossRef](#)]
20. Trindade, F.C.L.; Freitas, W.; Vieira, J.C.M. Fault Location in Distribution Systems Based on Smart Feeder Meters. *IEEE Trans. Power Del.* **2014**, *29*, 251–260. [[CrossRef](#)]
21. Hossan, S.; Chowdhury, B. Data-Driven Fault Location Scheme for Advanced Distribution Management Systems. *IEEE Trans. Smart Grid* **2019**, *10*, 5386–5396. [[CrossRef](#)]
22. Deng, W.; Pei, W.; Shen, Z.; Zhao, Z.; Qu, H. Adaptive Micro-Grid Operation Based on IEC 61850. *Energies* **2015**, *8*, 4455–4475. [[CrossRef](#)]
23. Liu, C.-H.; Gu, J.-C. Modeling and Integrating PV Stations into IEC 61850 XMPP Intelligent Edge Computing Gateway. *Energies* **2019**, *12*, 1442. [[CrossRef](#)]
24. Ishchenko, D.; Kondabathini, A.; Brissette, A.; Serra, P.; Baccino, F. Real-time hardware-in-the-loop modeling for mi-crogrid applications. In Proceedings of the 6th International Conference on Clean Electrical Power, Santa Margherita Ligure, Italy, 27–29 June 2017; pp. 152–157.